Survival of reactive carbon through meteorite impact melting

John Parnell
Paula Lindgren
Department of Geology, University of Aberdeen, Aberdeen AB24 3UE, UK

ABSTRACT

Melt fragments in melt breccias from the Gardnos impact crater, Norway, contain abundant carbon. A high proportion of the carbon present in the original melt was preserved. The stripping of hydrogen from carbon during melting prevents later hydrocarbon formation, hence the carbon is fixed in place rather than volatilized. Underlying lithic breccias that were not melted record hydrocarbon generation as a response to less extreme heating. Despite the high-temperature history of the melt, the carbon from the Gardnos impact crater is highly disordered, rather than ordered crystalline graphite, and in this respect, it is comparable with carbon in chondrite chondrules. Disordered carbon bears functional groups upon weathering, and, therefore, carbon preserved through impact or other melting may be available for reworking into biologically relevant organic molecules.

Keywords: Carbonaceous, chondrites, Gardnos crater, impact crater, meteorite, prebiotic chemistry.

INTRODUCTION

Meteorites and comets are thought to have been major agents of carbon flux to the surface of early Earth and other planets (Chyba and Sagan, 1997). Meteorite impact is also likely to substantially alter accumulations of organic molecules present at the surface (Maher and Stevenson, 1988). Consequently, there is strong interest in the fate of carbon during and following impact events, both in the impactor and in the target rocks, and in the implications for the availability of the carbon for prebiotic chemistry (Chyba and Sagan, 1997; Blank et al., 2001). As carbon is heated, it is progressively graphitized, so that its structural order is a measure of thermal alteration; this can be applied to both terrestrial and extraterrestrial materials (Rietmeijer and Mackinnon, 1985; Quirico et al., 2003). This response to temperature is well characterized due to extensive data sets from sedimentary basins and metamorphic terranes, where the carbon has been heated to 500+ °C (Wopenka and Pasteris, 1993). The response of carbon to much higher temperatures, including impact melting, is by contrast poorly understood. However, most of the carbon is assumed to be lost from the impact site during melting and devolatilization (Kieffer and Simonds, 1980). Carbon-rich melt fragments from the Gardnos impact crater, Norway, offer an opportunity to assess the degree to which carbon is preserved during impact events and its structural order.

CARBON DISTRIBUTION IN GARDNOS CRATER

Geological Setting

The Gardnos impact crater (Fig. 1) contains carbon-rich breccias (French et al., 1997; Gilmour et al., 2003). The age of impact is uncertain (see following discussion), but since the only candidate target rock with adequate carbon is the Cambrian Alum Shale (Gilmour et al., 2003), the impact is likely to have occurred during the 550–400 Ma interval between the Cambrian and the Caledonian orogeny, which overprinted the impact rocks with a metamorphic fabric at estimated temperature and pressure conditions of up to 400 °C and 2.5 kbar (Andersen and Burke, 1996). The Alum Shale was thermally immature at this time, and therefore it was rich in volatile organic compounds and water and had an exceptionally high organic carbon content, averaging 10% in the outcrops closest to Gardnos (Andersson et al., 1985). In addition to these sediments, the impact caused the melting of basement rocks including granites, gneisses, amphibolites, and quartzites. Above the impact-shocked basement are lithic breccias (Gardnos Breccia and Black Matrix Breccia of French et al., 1997), and suevite (breccia with melt particles) with lenses of melt-matrix breccia (Fig. 1). The suevite contains ~4% black melt fragments by volume, which was determined from two-dimensional (2-D) image analysis of 600 cm^2 and converted to three-dimensional values (note: consistent with ~12% by 2-D point counting). The black melt fragments occur in each of several exposures in the main suevite outcrop, building excavations, drill core, and till blocks. Each melt fragment consists of two immiscible phases (designated S, C) in variable proportions, now represented by the silicates stilpnomelane and chlorite, which reflect later alteration (Lindgren and Parnell, 2005). In younger deposits in other craters, the melt phases still consist of glass, but none remains at Gardnos. Delicate flow textures indicate that the Gardnos melt fragments were still liquid during deposition.

Carbon Precipitation in Suevite Melt

In 32 of 34 melt fragments examined, the boundary between the S and C phases is marked by a layer of carbon up to 20 μm thick (Fig. 2). The carbon also occurs at the boundary between the S phase and the host (nonmelt) matrix, but not between the C phase and the matrix. This indicates that the carbon precipitated from the S phase, and was consistently the first solid product that nucleated at the boundaries of the S phase. The observations were made on over 10 different

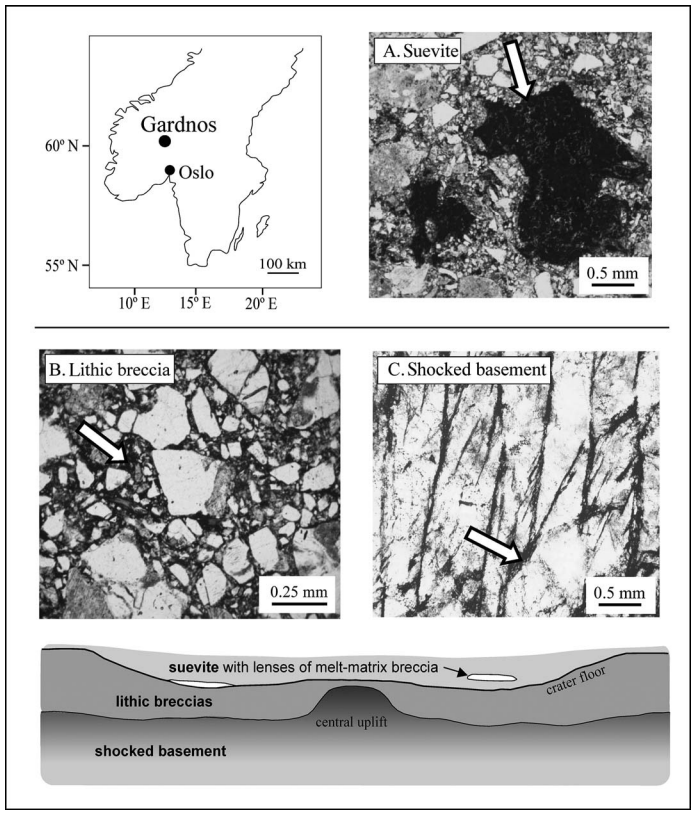

Figure 1. Location for Gardnos crater, and schematic cross section showing sequence of suevite (melt-bearing breccia) on lithic breccias, and basement of granitic gneiss, amphibolite, and quartzite. Photomicrographs show distinct forms of carbon distribution (black, arrowed) in (A) suevite, with carbon-rich melt fragments; (B) lithic breccia, with carbon-rich matrix, mostly in microfractures; and (C) basement quartzite, with carbon on deformation planes.

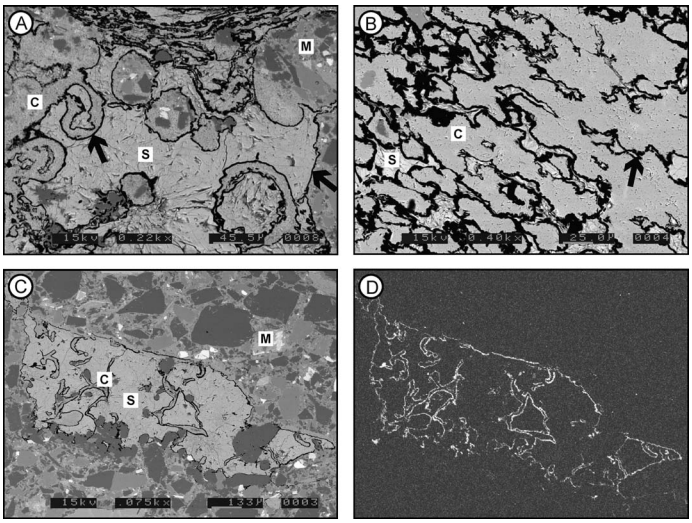

Figure 2. Backscattered-electron micrographs and X-ray map of carbon-rich melt fragments from Gardnos suevite, showing immiscibility textures, including intermingling tunnels with curved interfaces of phase C and phase S, and flow of two immiscible phases within each other. Carbon appears black (arrows) at contact between phase S and C, and between phase S and matrix (M), but not between phase C and matrix. A: Melt fragment with mingling between two phases S and C. Matrix, composed of angular lithic fragments, appears enclosed in melt fragment due to intersection of melt fragment in third dimension. B: Flow structures within melt fragment. C: Melt fragment with intermingling "tunnels" of phase C in phase S. D: X-ray map for carbon (white areas) corresponding to image C. Images were collected using scanning-electron microscope (ISI ABT-55) at 15 kV; X-rays were collected for 15 ms in 512 × 512 grids. Mapping at resolution 0.9 μm shows no carbon particles in S or C phase.

samples, mostly from till. Melt fragments were present in all samples, implying that they are widespread. Most melt fragments show fabric anisotropy due to compaction and melt flow, which has led to a range of immiscibility textures on 2-D surfaces (Lindgren and Parnell, 2005) that are highlighted by the carbon at the S/C boundary (Fig. 2). The melt-matrix breccias are mineralogically more complex (variable chloritoid, additional quartz, K-feldspar), but similarly show carbon layers at silicate-silicate phase boundaries. It is very unlikely that alteration of the glasses caused redistribution of the carbon, because the fine pattern of layers on phase boundaries is not disrupted. The melt from carbon-rich shales and granitic basement would have been silicate-dominated with a high volatile content (shales had 10+% organic carbon, typically several % water). Large amounts of carbon can dissolve in hydrous granitic melts (Korsakov et al., 2004), but carbon solubility in silicate melts decreases drastically over 1200–800 °C and is negligible (ppm level) at Earth surface temperatures (Pineau and Javoy, 1983). In impact craters where cooling, from 3000+ °C, was sufficiently fast to form abundant glass (Koeberl, 2002), solid carbon could precipitate on a widespread scale, as in the Gardnos melt. It is probable that the current mineralogy of the two phases reflects a distinction in the chemistry of the two immiscible melt phases, where stilpnomelane represents a melt phase with higher silica content than the chlorite precursor. Carbon solubility in aluminosilicate melts increases with silica content (Park and Min, 2000), which is consistent with carbon fractionation into the S phase at Gardnos.

An alternative origin for the carbon as a residue of hydrocarbon migration can be discounted because (1) the carbon only occurs at the S to matrix boundary but never at the C to matrix boundary, (2) there is no carbon in more accessible sites, such as fractures crosscutting mineral fragments in the melt breccia (fractures in lithic breccia and basement *are* filled; see following), and (3) stringers of melt extending from the melt fragments contain carbon out to their tips, precluding later emplacement. Furthermore, it would be physically impossible to emplace the carbon into glass fragments as migrating hydrocarbons. Heavy oil is much too viscous to thoroughly impregnate an extensive tortuous micron-scale network, even if the permeability was much higher than at present. Oil fine enough to enter the network could only produce a limited amount of heavy compounds as a solid degradation product. Thus, the continuous carbon layers at the S to matrix interface cannot be a product of later fluids.

The suevite is crosscut by veinlets of hydrothermal quartz that contain micron-scale hydrocarbon fluid inclusions. The inclusions also occur in healed microfractures through quartz fragments and basement clasts.

The response of hydrocarbon source rocks to flash heating must show a gradation with intensity of heating. With decreasing intensity, the response will range through vaporization, melting, carbonization and graphitization, hydrocarbon generation, and lesser degrees of thermal maturation. These effects will be manifest in different parts of a crater system. At Gardnos, the identifiable products are carbon-bearing melt and hydrocarbons. While melt is generated almost instantaneously upon impact, hydrocarbon generation is kinetically controlled and will occur during postimpact hydrothermal activity. The result at Gardnos is suevite, containing carbon-rich melt fragments (Fig. 1B), crosscut by hydrothermal quartz veins and healed microfractures, containing hydrocarbon fluid inclusions. The lithic breccias and basement below the suevite also contain hydrocarbon fluid inclusions and associated solid residues of hydrocarbons (Fig. 1C). The solid residues are particularly evident in shocked quartzite (Fig. 1D), where they occupy microfractures attributed by Andersen and Burke (1996) to the impact event. Microfractures through quartz heal rapidly (Brantley, 1992), implying that the hydrocarbon inclusions and carbonaceous residues were entrained during hydrothermal activity immediately postimpact rather than at a later time.

Carbon Content

X-ray maps show that the carbon is strongly localized at mineral phase boundaries within the melt fragments (Fig. 2). The carbon distribution is confirmed by mean carbon contents for whole melt fragments and the matrix of 5.2 ± 2.0% (n = 20, from 14 different samples) and 0.3 ± 0.06% (n = 10), respectively, which were determined using a LECO CS225 carbon analyzer. These values are consistent with bulk carbon values in the suevite of 0.6 ± 0.01% (n = 5) and the carbon-bearing melt volume of 4%. Analyses of unmelted basement clasts yield a mean carbon content of 0.3 ± 0.07% (n = 10), which is comparable with the matrix content, i.e., the basement fragments do not contain an enrichment in carbon. The S and C phases in the melt cannot be physically separated for analysis, but energy dispersive X-ray analysis shows no detectable carbon ($<\sim$0.1%) within the mineral phases, but solely carbon in the boundary layers. To confirm this, laser Raman spectroscopy shows very strong responses for carbon in the boundary layer but no carbon in the S/C phases (Fig. 3). The lack of carbon in the melt silicate phases reflects the very low solubility of carbon in glasses (Pineau and Javoy, 1983), which would have caused the carbon to precipitate first. The X-ray maps suggest that the limited carbon contents measured in the matrix represent micron-scale melt stringers. Carbon in the basement fragments occurs in healed microfractures. However, the carbon content varies even between adjacent melt fragments, showing that the melt was not homogeneous. The concentration of the carbon in the melt implies that although the suevite breccias were derived from a mixture of carbon-rich shale and crystalline basement (Gilmour et al., 2003), the shale component was largely incorporated into the melt; i.e., there was a disproportionate incorporation of the volatile-rich sedimentary target into the melt, as predicted on theoretical grounds (Kieffer and Simonds, 1980). Accord-

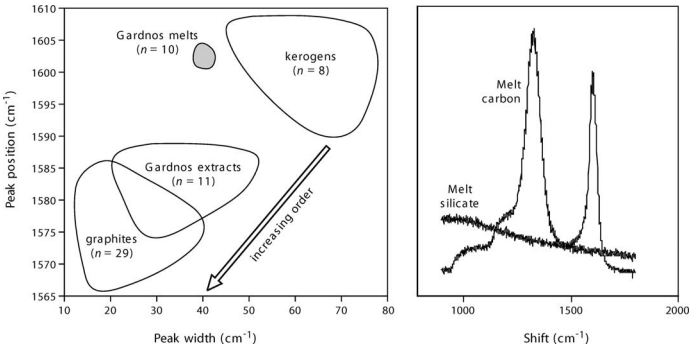

Figure 3. Characterization of carbon in Gardnos melt fragments by Raman spectroscopy cross-plot of O (order) peak position and O peak width (half-height). Graphite and kerogen fields are from Wopenka and Pasteris (1993). Melt carbon is disordered, similar to kerogen. Gardnos acid-extract data (Gilmour et al., 2003) represent a minor component of carbon in suevites. Sample spectrum is shown for carbon and stilpnomelane in melt fragment. Stilpnomelane shows no response for carbon, which suggests that ≪1% could be present. Raman spectroscopy was performed using a Jobin-Yvon Labram laser Raman microprobe by R. Court at The Open University. Excitation was provided by a 40 mW, 514.5 nm, Ar-ion laser, delivering around 8 mW to thin sections. Spectra were obtained using a 25× objective and a 600 grids mm^{-1} grating.

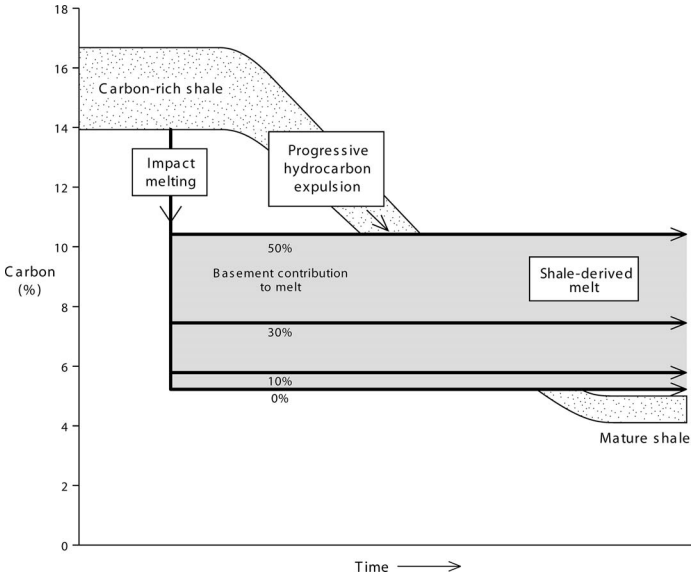

Figure 4. Comparison of carbon loss from Alum Shale by impact melting and progressive hydrocarbon generation. Initial carbon content range is extrapolated from current values of 10%–12%, assuming 0.4 expulsion efficiency (Cornford, 1998). There was no carbon loss before impact because Alum Shale was thermally immature (Andersson et al., 1985), so it had not generated hydrocarbons. Carbon loss by hydrocarbon generation follows model for oil-prone kerogen achieving full maturity (Cornford, 1998). Carbon percentage in shale-derived melt is shown for a range of basement contributions to melt.

ingly, we found no unmelted shale, whereas basement fragments exhibit only partial melting.

Characterization of Carbon

The Gardnos carbon exhibits a strong degree of disorder (Fig. 3). The Raman D/O intensity ratio is equivalent to an in-place crystallite dimension (La) of 13 Å, indicating very poor crystallization (Wopenka and Pasteris, 1993). This disordered material represents the bulk of the carbon in the rock and is distinct from highly ordered graphite and diamond recorded by Gilmour et al. (2003), which are trace components in the same rocks (Fig. 3). The O (order) peak is displaced from the ordered graphite position at 1585 cm^{-1} to 1602 cm^{-1} due to merging with a disorder peak at 1620 cm^{-1}. Similar displacement and disorder are observed in the products of experimental carbon-rich silicate melts (Kadik et al., 2004). However preexisting carbon can survive metamorphism in a relatively disordered state (e.g., Pitcairn et al., 2005). If the carbon had been precipitated due to crystallization during metamorphism, it would occur as ordered graphite crystals (Luque et al., 1998), which are not evident.

DISCUSSION

Implications for Geothermometry and Cosmothermometry

The degree of structural order in carbonaceous materials is widely used as a geothermometer. The relationship between order and temperature has also been extended to extraterrestrial samples and invoked as a cosmothermometer, applied to chondrites and interplanetary dust particles (Rietmeijer and Mackinnon, 1985; Brearley, 1990). In terrestrial metamorphic rocks, fully ordered graphite is achieved by 450–600 °C (Rietmeijer and Mackinnon, 1985). Poorly graphitized carbon in extraterrestrial materials is therefore commonly attributed to processing at lower temperatures, with consequences for their inferred origin (Brearley, 1990; Quirico et al., 2003). However, carbon precipitated from a cooling melt has not experienced the gradual development of structural order found in progressively heated samples. Hence, despite a melt temperature that was probably well in excess of 1000 °C, the Gardnos carbon is disordered. Similarly, disordered carbon is a product of experimental silicate melts (Kadik et al., 2004). Disorder cannot therefore be used as a geothermometer, or cosmothermometer, where carbon is precipitated directly at high temperature.

The disorder in melt products explains the occurrence of poorly graphitized carbon in chondrite chondrules, which have experienced melting at 1500+ °C (Mostefaoui et al., 2000). There are several similarities between carbon processed in the chondrules and carbon in the Gardnos impact melt, in which the precursors were (1) carbon-rich, (2) macromolecular solids that were (3) hydrogenated, (4) combined with silicates, and (5) melted (Hanon et al., 1998). Experimental manufacture of chondrules by flash heating incorporated up to 10% carbon in a silicate melt, and although some carbon is preserved after quenching, much is lost by redox reactions with iron silicates (Connolly et al., 1994; Hanon et al., 1998). The high degree of carbon preservation in Gardnos may reflect lower iron contents in sediment-derived melts compared with the olivine-rich chondrules.

Preservation of Carbon

Adopting an average 10% carbon content for the Alum Shale (Andersson et al., 1985), the melt represents preservation of a high proportion of the original carbon. We estimate 0.4 expulsion efficiency of oil from the Alum Shale, which equates to an original carbon content of 13.9% (Cornford, 1998), which in turn implies a preservation of at least 38% carbon in the melt. If the melt contains a significant proportion of granitic basement or noncarbonaceous sediments, the percentage carbon preservation is even higher. Basement contributions of 10%, 30%, and 50% equate to 42%, 54%, and 75% carbon preservation (Fig. 4). Adopting the maximum regional carbon content for the Alum Shale of 12% (Andersson et al., 1985) and a lower measured value of 7.4% (Gilmour et al., 2003) adjusted to initial values of 16.7% and 10.3% yields absolute minimum levels of carbon preservation in the melt from 31% to 51%. These estimates represent a lower loss of carbon from shales than occurs during the generation of hydrocarbons during burial, where ''hydrogen balance'' calculations (Cornford, 1998) indicate that oil-prone, hydrogen-rich organic matter like that in the Alum Shale is depleted to 30% of the original carbon (Fig. 4). Hydrocarbon generation is kinetically inhibited during geologically instantaneous impact melting, and there is minimal opportunity for oxidation of the carbon to gaseous species. However, hydrogen would be stripped

from the organic carbon during melting, and instead form dissolved OH^-, H_2O, and H_2 in the melt (Kadik et al., 2004). Such hydrogen redistribution would prevent later carbon loss by hydrocarbon generation.

A postulated alternative source for carbon, the Proterozoic Biri Shale with maximum content of 1.66% (Gilmour et al., 2003) is quite incompatible with the carbon content of the melt fragments, without adopting an unidentified process by which carbon is concentrated by over 300%. This strongly implies that the Alum Shale is the true target rock.

Implications for Extraterrestrial Carbon

The abundant carbon in silicate melt fragments has implications for the preservation of carbon in interplanetary materials. Silicate melting is evident in carbon-bearing interplanetary dust particles (Brownlee et al., 1997), chondrite chondrules (Hanon et al., 1998), and on the parent body of some carbon-rich meteorites (Cohen et al., 2004). Indeed, the parent body of all carbonaceous chondrites may experience melting during impact events. Carbon in these materials could survive devolatilization by incorporation into melts, but also survive conversion into refractory or highly ordered forms. On asteroids, carbon-rich melts may devolatilize readily by degassing (Scott et al., 1993). However the evidence from Gardnos indicates that reduced carbon can survive oxidation to volatile gases within silicate melts, and is therefore retained in elemental form.

The host glass in an impact melt is mineralogically unstable and would weather readily to release the carbon to become incorporated in the planetary regolith. Poorly ordered carbon exposed to the atmosphere bears functional groups on the surface (Simpson and Hatcher, 2004), making it reactive and bioavailable. Bombardment of the planetary regolith by energetic H^+ ions could also cause hydrogenation (Starukhina and Shkuratov, 1995). We conclude that carbon processed through impact melts is not simply converted to an inert (highly crystalline) form or destroyed (Kieffer and Simonds, 1980), but can survive in substantial proportions for further processing in prebiotic chemistry or by primitive life.

ACKNOWLEDGMENTS

We thank R. Court and J. Still for skilled technical help, and G. Osinski, H. Dypvik, and M. Sephton for helpful criticism.

REFERENCES CITED

Andersen, T., and Burke, E.A.J., 1996, Methane inclusions in shocked quartz from the Gardnos impact breccia: South Norway: European Journal of Mineralogy, v. 8, p. 927–936.

Andersson, A., Dahlman, B., Gee, D.G., and Snäll, S., 1985, The Scandinavian Alum Shales: Sveriges Geologiska Undersökning, Ca, v. 56, p. 1–50.

Blank, J.G., Miller, G.H., Ahrens, M.J., and Winans, R.E., 2001, Experimental shock chemistry of aqueous amino acid solutions and the cometary delivery of prebiotic compounds: Origins of Life and Evolution of the Biosphere, v. 31, p. 15–51, doi: 10.1023/A:1006758803255.

Brantley, S.L., 1992, The effect of fluid chemistry on quartz microcrack lifetimes: Earth and Planetary Science Letters, v. 113, p. 145–156, doi: 10.1016/0012-821X(92)90216-I.

Brearley, A.J., 1990, Carbon-rich aggregates in type-3 ordinary chondrites—Characterization, origins, and thermal history: Geochimica et Cosmochimica Acta, v. 54, p. 831–850, doi: 10.1016/0016-7037(90)90377-W.

Brownlee, D.E., Joswiak, D., and Bradley, J.P., 1997, Vesicular carbon in strongly heated IDPs: Houston, Texas, Lunar and Planetary Science Conference XXVIII, abstract 1585.

Chyba, C., and Sagan, C., 1997, Comets as a source of prebiotic organic molecules for the early Earth, *in* Thomas, P.J., Chyba, C.F., and McKay, C.P., eds., Comets and the Origin and Evolution of Life: New York, Springer, p. 147–173.

Cohen, B.A., Goodrich, C.A., and Keil, K., 2004, Feldspathic clast populations in polymict ureilites: Stalking the missing basalts from the ureilite parent body: Geochimica et Cosmochimica Acta, v. 68, p. 4249–4266, doi: 10.1016/j.gca.2004.01.027.

Connolly, H.C., Hewins, R.H., Ash, R.D., Zanda, B., Lofgren, G.E., and Bourotdenise, M., 1994, Carbon and the formation of reduced chondrules: Nature, v. 371, p. 136–139, doi: 10.1038/371136a0.

Cornford, C., 1998, Source rocks and hydrocarbons of the North Sea, *in* Glennie, K.W., ed., Petroleum Geology of the North Sea (4th ed.): Oxford, Blackwell, p. 376–462.

French, B.M., Koeberl, C., Gilmour, I., Shirey, S.B., Dons, J.A., and Naterstad, J., 1997, The Gardnos impact structure, Norway: Petrology and geochemistry of target rocks and impactites: Geochimica et Cosmochimica Acta, v. 61, p. 873–904, doi: 10.1016/S0016-7037(96)00382-1.

Gilmour, I., French, B.M., Franchi, I.A., Abbott, J.I., Hough, R.M., Newton, J., and Koeberl, C.I., 2003, Geochemistry of carbonaceous impactites from the Gardnos impact structure, Norway: Geochimica et Cosmochimica Acta, v. 67, p. 3889–3903, doi: 10.1016/S0016-7037(03)002130-8.

Hanon, P., Robert, F., and Chaussidon, M., 1998, High carbon concentrations in meteoritic chondrules: A record of metal-silicate differentiation: Geochimica et Cosmochimica Acta, v. 62, p. 903–913, doi: 10.1016/S0016-7037(97)00385-2.

Kadik, A., Pineau, F., Litvin, Y., Jendrzejewski, N., Martinez, I., and Javoy, M.A., 2004, Formation of carbon and hydrogen species in magmas at low oxygen fugacity: Journal of Petrology, v. 45, p. 1297–1310, doi: 10.1093/petrology/egh007.

Kieffer, S.W., and Simonds, C.H., 1980, The role of volatiles and lithology in the impact cratering process: Reviews of Geophysics and Space Physics, v. 18, p. 143–181.

Koeberl, C., 2002, Mineralogical and geochemical aspects of impact craters: Mineralogical Magazine, v. 66, p. 745–768, doi: 10.1180/0026461026650059.

Korsakov, A.V., Theunissen, K., and Smirnova, L.V., 2004, Intergranular diamonds derived from partial melting of crustal rocks at ultrahigh-pressure metamorphic conditions: Terra Nova, v. 16, p. 146–151, doi: 10.1111/j.1365-3121.2004.00547.x.

Lindgren, P., and Parnell, J., 2005, Liquid immiscibility in suevite melt, Gardnos impact crater: Houston, Texas, Lunar and Planetary Science Conference XXXVI, abstract 1629.

Luque, F.J., Pasteris, J.D., Wopenka, B., Rodas, M., and Barrenechea, J.F., 1998, Natural fluid-deposited graphite: Mineralogical characteristics and mechanisms of formation: American Journal of Science, v. 298, p. 471–498.

Maher, K.A., and Stevenson, D.J., 1988, Impact frustration of the origin of life: Nature, v. 331, p. 612–614, doi: 10.1038/331612a0.

Mostefaoui, S., Perron, C., Zinner, E., and Sagon, G., 2000, Metal-associated carbon in primitive chondrites: Geochimica et Cosmochimica Acta, v. 64, p. 1945–1964, doi: 10.1016/S0016-7037(99)00409-3.

Park, J.H., and Min, D.J., 2000, Thermodynamic behaviour of carbon in molten slags: Iron and Steel Institute of Japan International, v. 40, p. S96–S100.

Pineau, F., and Javoy, M., 1983, Carbon isotopes and concentrations in mid-oceanic ridge basalts: Earth and Planetary Science Letters, v. 62, p. 239–257, doi: 10.1016/0012-821X(83)90087-0.

Pitcairn, I.K., Roberts, S., Teagle, D.A.H., and Craw, D., 2005, Detecting hydrothermal graphite deposition during metamorphism and gold mineralization: Journal of the Geological Society of London, v. 162, p. 429–432, doi: 10.1144/0016-764904-139.

Quirico, E., Raynal, P.-I., and Bourot-Denise, M., 2003, Metamorphic grade of organic matter in six unequilibrated ordinary chondrites: Meteoritics & Planetary Science, v. 38, p. 795–811.

Rietmeijer, F.J.M., and Mackinnon, I.D.R., 1985, Poorly graphitised carbon as a new cosmothermometer for primitive extraterrestrial materials: Nature, v. 315, p. 733–736, doi: 10.1038/315733a0.

Scott, E.R.D., Taylor, G.J., and Keil, K., 1993, Origin of ureilite meteorites and implications for planetary accretion: Geophysical Research Letters, v. 20, p. 415–418.

Simpson, M.J., and Hatcher, P.G., 2004, Determination of black carbon in natural organic matter by chemical oxidation and solid-state ^{13}C nuclear magnetic resonance spectroscopy: Organic Geochemistry, v. 35, p. 923–935, doi: 10.1016/j.orggeochem.2004.04.004.

Starukhina, L.V., and Shkuratov, Y.G., 1995, A model for ion bombardment-induced organic synthesis on carbon-bearing surfaces in cosmic space: Icarus, v. 113, p. 442–449, doi: 10.1006/icar.1995.1033.

Wopenka, B., and Pasteris, J.D., 1993, Structural characterization of kerogens to granulite-facies graphite: Applicability of Raman microprobe spectroscopy: The American Mineralogist, v. 78, p. 533–557.

Manuscript received 3 March 2006
Revised manuscript received 4 July 2006
Manuscript accepted 13 July 2006

Printed in USA